To Mol Nutrition and Food Res.

Sulforaphane regulates abnormal lipid metabolism via both ERS-dependent XBP1/ACC &SCD1 and ERS-independent SREBP/FAS pathways

Sicong Tian[1,#], Baolong Li[2,#], Peng Lei[1], Xiuli Yang[1], Xiaohong Zhang[3,*], Yongping Bao[4,*], Yujuan Shan[1,*]

[1]Department of Food Science and Engineering, School of Chemistry and Chemical Engineering, Harbin Institute of Technology, Harbin 150090, China.

[2]Heilongjiang University of Chinese Medicine, Harbin, 150040, China.

[3]Institute of Preventative Medicine and Zhejiang Provincial Key Laboratory of Pathological and Physiological Technology, School of Medicine, Ningbo University, Zhejiang, 315211, China.

[4]Norwich Medical School, University of East Anglia, Norwich NR4 7UQ UK.

[#]Contributed equally to this work

[*]Corresponding author

Abbreviations

4-PBA	4-Phenyl Butyric Acid
ACC1	Acetyl CoA Carboxylase 1
ERS	Endoplasmic Reticulum Stress
FAS	Fatty Acid Synthase

Received: 25-Aug-2017; Revised: 14-Jan-2018; Accepted: 17-Jan-2018

This article has been accepted for publication and undergone full peer review but has not been through the copyediting, typesetting, pagination and proofreading process, which may lead to differences between this version and the Version of Record. Please cite this article as doi: 10.1002/mnfr.201700737.

IRE1	Inositol-requiring Enzyme-1
LDs	Lipid Droplets
NAFLD	Non-alcoholic Fat Liver Disease
PERK	Protein Kinase-like ER Kinase
PPC	Polyene Phosphatidylcholine
SCD1	Stearoyl-CoA Desaturase 1
SFN	Sulforaphane
SREBP-1c	Sterol Regulatory Element Binding Protein-1c
TC	Cholesterol
TG	Triglyceride
UPR	Unfolded Protein Response
XBP1	X-Box Binding Protein 1
HFD	High Fat Diet
VLDL	Very-Low-Density Lipoproteins
HMGCS	HMG-CoA synthase
HMGCR	HMG-CoA reductase

Keywords: sulforaphane; lipid metabolism; sterol regulatory element binding protein-1c; endoplasmic reticulum stress; lipogenic enzymes

Abstract

Scope: To investigate the effect of sulforaphane (SFN) on the abnormal lipid metabolism and underlying mechanisms.

Methods and results: Models with abnormal lipid metabolism were established both in rats and human hepatocytes. Hepatic steatosis was detected by H&E and oil red O staining. The structure of endoplasmic reticulum was visualized by transmission electron microscopy. The expressions of X-box binding protein 1 (XBP1), protein kinase-like ER kinase (PERK), sterol regulatory element binding protein-1c (SREBP1c) and lipogenic enzymes were determined by real-time PCR and western blot analysis. SFN lowered the content of triglyceride and cholesterol. SFN alleviated the swelling of endoplasmic reticulum (ER) and decreased the perimeter of ER. SFN significantly decreased the expressions of acetyl CoA carboxylase 1 (ACC1), stearoyl-CoA desaturase 1 (SCD1) and fatty acid synthase. SFN inhibited SREBP1c by blocking the PERK. Meanwhile, SFN suppressed ACC1 and SCD1 via blocking the formation of splicing-type XBP1. The key roles of XBP1 and SREBP1c in SFN-reduced lipid droplets were confirmed by a timed sequence of measurement according to time points.

Conclusion: SFN improved abnormal lipid metabolism via both ER stress -dependent and -independent pathways.

Introduction

The Westernization of dietary patterns in China may lead to the excessive intake of fats and accumulation of lipids in the body which can cause non-alcoholic fat liver disease (NAFLD), diabetes, obesity, cardiovascular disease, atherosclerosis, *etc*. [1-2]. In addition to the physical activities, the dietary habit is more critical way to be adjusted. NAFLD, characteristic of hepatic lipid accumulation, results from an imbalance between lipid synthesis, storage, oxidation, and/or secretion, and eventually triggers hepatitis hepatocirrhosis and even hepatoma [3]. Lipids such as triglyceride (TG) and cholesterol (TC) are stored in the form of lipid droplets (LDs) in hepatocytes. Lipids are synthesized in the endoplasmic reticulum (ER) together with the folding of membrane proteins and secretory proteins. An overload of unfolded or misfolded proteins may result in excessive fatty acids retention in the ER followed by the ER stress (ERS) which in turn aggravates the lipid accumulation. Long term lipid accumulation in the non-adipose cells i.e. hepatocytes, could exceed the capacity of the cells to manage lipids and cause further chronic ERS and lipotoxicity [4].

Mono-unsaturated fatty acids have the ability to attenuate acute ERS induced by palmitate, while excess fatty acid exposure over long periods of time can exceed the capacity, especially of non-adipose cells. For example, short-term treatment of cells with oleic acid increases very-low-density lipoproteins (VLDL) and triglyceride secretion, whereas prolonged incubation of cells with oleic acid can lead to ERS and of VLDL secretion [5].

When ERS occurs, the ER initiates the unfolded protein response (UPR) through the actions of canonical sensors IRE1, PERK, and ATF6 to restore ER homeostasis. The excessive accumulation of unfolded or misfolded proteins stimulates the ERS sensors to uncouple from GRP78 [6-7]. Among these sensors, IRE1 a ribonuclease that splices uXBP1 transcripts into the active sXBP1. Then sXBP1 is translocated into the nucleus to promote the transcription of lipogenic enzymes such as acetyl-CoA carboxylase 1 (ACC1) and stearoyl-CoA desaturase 1 (SCD1) [8]. In addition, PERK regulates fatty acid synthase (FAS) via sterol regulatory element binding protein-1c (SREBP1c) [9].

In the past few decades, plant-derived bioactives have been demonstrated to have the potential to prevent lipids-associated disorders. An epidemiological study involving 1938 healthy adults showed that intake of adequate phytochemicals was beneficial, lowering body weight and body fat [10]. Sulforaphane (SFN), an isothiocyanate found in cruciferous vegetables, especially in broccoli, was reported to regulate a number of metabolic enzymes including phase I & phase II metabolic enzymes, and lipid metabolism-related enzymes/proteins [11]. Oral administration of the sulfur-radish extract and of sulforaphane after carbon tetrachloride (CCl_4)-induced liver injury both decreased the serum level of alanine aminotransferase reduced the necrotic zones, inhibited lipid peroxidation, and induced phase 2 enzymes without affecting cytochrome P450-2E1 (CYP2E1). [12]. Moreover, long-term consumption of whole broccoli counters NAFLD development enhanced by a Western diet as well as hepatic tumorigenesis induced by DEN in B6C3F1 mice. [13] Therefore, we further hypothesized that SFN presents a preventive effect on the abnormal lipid metabolism via ERS mechanisms. In the present study, high-lipid induced abnormal lipid metabolism models were established both *in vitro* and *in vivo* to explore the protective effects of SFN and focusing on the ER-dependent/independent mechanisms.

Material and Method

2.1 Reagent and Preparation

Sulforaphane (1-isothiocyanato-4-(methylsulfinyl) butane, SFN, purity≥98%), purchased from LKT laboratories (St. Paul, MN), stock solution (100 mmol/L) was prepared in dimethyl sulfoxide (DMSO) and stored -20^{o}C. 4-phenyl butyric acid (4-PBA) was purchased from Sigma-Aldrich (Saint Louis, USA). Antibodies against SREBP-1c, XBP1, lamin B were from Proteintech Biotechnologies (USA). Antibody against PERK was from Santa Cruz Biotechnology (USA). TRIZOL reagent kit, TransScript One-Step gDNA Removel and cDNA Synthesis SuperMix kit, TransStart Top Green qPCR SuperMix kit were purchased from TransGen Biotech (China). Kits for measuring triglycerides and cholesterol were purchased from Nanjing Jiancheng Biotechnologies (China). The animal chow was purchased from Keaoxieli Feed Co., Ltd (Beijing, China). Polyene Phosphatidylcholine (PPC) was purchased from Pharmacy (China) and dissolved in soya-bean oil.

Oleic acid and palmitic acid were bought from Sigma-Aldrich (Saint Louis, USA). Palmitic acid was prepared as described previously [14]. Briefly, palmitate and oleate were dissolved in 0.1 mol/L NaOH at 70^{o}C and filtered respectively to prepare 100 mmol/L palmitate stocks and 100 mmol/L oleate stocks. Five percent (w/v) FFA-free BSA (Sigma) solution was prepared in double-distilled H_2O. 100 mmol/L FA and 5% BSA solution were mixed by 1:1 (v/v) in at 60℃and filtered.

2.2 Cell Culture and Treatment

Immortalized human hepatocytes (defined as HHL-5) were kindly supplied by Professor Arvind Petal, Medical Research Council (MRC) Virology Unit, UK. HHL-5 hepatocytes were cultured in DMEM/F12 (1:1) medium with 10% fetal bovine serum, at 37^{o}C and 5% carbon dioxide. After reaching 70% confluence, cells were pre-treated with SFN once (1, 5, 10, 20 μmol/L) for 24 h, followed by 0.25 mmol/L FAs (oleic acid: palmitic acid, 2:1) for 5 days.

2.3 Establishment of NAFLD Animal Model and Treatments

All the procedures were conducted in conformity with the guidelines of the Institutional Animal Care Use Committee, Heilongjiang province, China. The protocols were approved by the Ethics Committee of Experimental Animals (Qualified number: SCXK-Hei-2012-023) at Heilongjiang University of Chinese Medicine.

Male Wistar rats (weighing 160-200 g, 4-6 weeks), specified as pathogen free, were obtained from The Center of Safety and Evaluation of Drugs, Heilongjiang University of Chinese Medicine. Animals were divided into 6 groups (n=10) and housed in a controlled-environment (temperature 22 ± 2°C and humidity 55 ± 5% with 12/12 h light and dark cycle) with free access to food and water. The formula of the diet is shown in Table 1.

NAFLD models were established using a high-fat diet (HFD) for 10 weeks. Rats in the control group were given normal diet. The HFD contains 24% fat, 24% protein and 41% carbohydrate (a percentage of total kcal, according to D12451; Research Diets Inc.) while the normal chow consisted of 7% fat, 24% protein and 64% carbohydrate (according to D10012G; Research Diets Inc). Six groups were classified in the animal experiments and the detail treatments in each group were summarized in Figure1. Polyene Phosphatidylcholine (PPC) is used as positive group (30 mg/kg), which has been widely applied in clinical to treat alcohol-induced hepatic fibrosis, hepatocyte steatosis, and nonalcoholic steato- hepatitis. Three doses of SFN (5 mg/kg, 10 mg/kg and 20 mg/kg) or PPC (30 mg/kg) were orally gavaged to rats 3 times a week along with HFD diet. The animal experimental scheme is totally shown in figure 1.

2.4 Measurement of Lipid Contents

To determine the TG and TC levels, blood samples were collected from abdominal aorta and centrifuged at 3000g for 15 min to obtain serum; liver samples were washed with PBS and lipids were extracted by homogenizing before spinning down. Cultured cells were washed twice with cold PBS and collected. Cellular lipids were extracted by homogenizing. After centrifugation, the supernatants were stored at -80°C before use. The TG and TC levels were measured using TG and TC kit (Nanjing, China) following the manufacturer's instructions and denoted as micrograms of lipid per milligram of cellular protein.

2.5 Oil Red O staining for LDs

Intracellular neutral lipid deposition was stained by Oil-red O. In brief, cultured hepatocytes were washed with ice-cold PBS twice, fixed with 4% paraformaldehyde at 4°C for 1 h, and stained with 0.2% Oil-red O in isopropanol for 10 min. The cells were then washed with 60% isopropanol and followed by visualization under the light microscope.

2.6 Pathological examination of liver

Liver sections were fixed in 4% paraformaldehyde solution for 24h and sent to the Department of Pathology, Heilongjiang University of Chinese Medicine for slide preparation and hematoxylin-eosin staining. The slides were reviewed in a blinded fashion by 3 pathologists from Heilongjiang University of Chinese Medicine, and were assigned an average histological score [15]. A slight modification was made to this scoring system: scores were multiplied the percentage of the total area affected and it is 0.5 if the ratio is less than 5%. Photographs were analysed using Image J software to determine the number of LDs.

2.7 The ER structure examined by transmission electron microscope

Transmission electron microscopy was performed [16]. Briefly, samples were fixed with 3% glutaraldehyde, post-fixed in osmium tetroxide, dehydrated with a graded acetone series, and finally embedded in Epon. Ultrathin sections were stained with uranyl acetate and lead citrate, examined in a JEM 1220 transmission electron microscope operated at 80 kV. Free hand selection was used to calculate the perimeter of ER from an average of 3 pictures in each experimental group (from 3 different animals per group) through Image J software according to Hotamisligil's method and all data are mean ± SEM, *P <0.05 [17].

2.8 Total RNA Extraction and Real-Time PCR analysis

Total RNA was extracted using TRIZOL reagent kit (TransGen Biotech, China) and quantified by measuring optical density at 260 nm and 280nm. cDNA was synthesized by Transcript One-Step g DNA Removal and cDNA Synthesis SuperMix kit (TransGen Biotech, China) according to the manufacturer's protocol. The first strand obtained was quantified by real-time quantitative PCR using a Passive Reference Dye I (50×) assay on an ABI Prism 7300 System (Applied Biosystems, CA). The PCR cycle conditions were 94℃ for 31 s, then 40 cycles at 94℃ for 5 s and 60 ℃ for 30 s. PCR primers for liver tissue and human hepatocytes were shown in Table 2 and Table 3 [8, 18-19].

2.9 Extraction of nuclear protein and western blot analysis

Nuclear proteins from cells and total proteins from animal liver were extracted using Protein Ext™ Mammalian Nuclear kit and Cytoplasmic Protein Extraction Kit (TransGen Biotech, China), respectively. Equal amounts of protein (40-60 μg) were separated on 5% to 10% SDS−PAGE and transferred to polyvinylidene difluoride (PVDF) membranes (Millipore, Bedford, MA). The membrane was blocked with 5% nonfat milk for 30 min at room temperature and then incubated with primary antibody (at 4 °C overnight), and followed by the secondary antibody labelled with alkaline phosphatase (at room temperature for 30 min). The membrane was then incubated with the secondary alkaline phosphatase-conjugated IgG and detected with Western Blue Stabilized Substrate for alkaline phosphatase (Promega). The relative densities of the individual bands were analyzed by densitometry using the ChemiImager 4000 (Alpha Innotech, USA).

2.10 Statistical Analysis

Results are expressed as means ± SEM. SPSS 19.0 software was used for statistical analysis. Statistical significance of difference was determined using one way ANOVA followed by multiple comparisons with a Tukey's test. *P <0.05 was considered to be significant.

Results

3.1 SFN attenuated TG and TC accumulation both *in vitro* and *in vivo*

To verify whether SFN could improve the lipid accumulation, a NAFLD animal model was established in rats, and TG and TC contents in serum were measured. As is shown in Fig. 2A, SFN decreased the content of TG and TC in a dose-dependent way. The levels of TG (1.2 mmol/L) and TC (2.6 mmol/L) were reduced to 0.71 mmol/L and 1.9 mmol/L, respectively by SFN (20 mg/kg).

Meanwhile, the content of TG and TC in liver presented the similar trend (Fig. 2B). Pathological examination of livers revealed that many more LDs, characterized as white round vacuoles, accumulated in HFD-rats (Fig. 2C, arrow indicated). SFN (5-20 mg/kg) and PPC (30mg/kg) treatments lessened the lipid accumulation seen as white LDs and histological steatosis is represented by the histological score in Fig. 2D.

To explore its underlying mechanisms, a cellular model of abnormal lipid metabolism induced by FA was developed in immortalized human hepatocytes HHL-5. FA-induced LDs, stained with oil red O, were examined under light microscopy (Fig. 2E, FA group, arrow position). In contrast to treatment with FA alone, HHL-5 cells incubated with SFN (10 μmol/L) had fewer lighter stained areas (Fig. 2E, SFN+FA group) suggesting that SFN disturbs the formation and distribution of LDs. The intracellular TG and TC contents were significantly reduced by treatment with SFN (Fig. 2F).

3.2 SFN decreases the lipogenic enzymes via activating the transcription factor-SREBP1c and XBP1

In general, the synthesis of TG and TC in liver is controlled by a series of endogenous lipogenic enzymes such as ACC1, FAS, and SCD1. HFD increased the expressions of ACC1, FAS and SCD1 mRNA by nearly 2-fold in comparison to normal diet group (Fig 3A). High doses of SFN downregulated the expressions of these enzymes as effectively as PPC, an efficient lipid-lowering drug (Fig 3A). The inhibitory effects of SFN on ACC1, FAS, and SCD1 mRNA expressions were also confirmed in FA-treated HHL-5 cells (Fig.3B).

Moreover, a transcription factor-SREBP1c, responsible for the transcription of lipogenesis-related enzymes, was further determined both in FA-induced HHL-5 cells and NAFLD rats. SFN treatment attenuated the expressions of SREBP1c mRNA (Fig. 3C) and SREBP1c protein in rat liver (Fig. 3D) with comparable effects to PPC treatment. Similarly, in the FAs-induced cell model, SFN (10 μmol/L and 20 μmol/L) lowered the expression of SREBP1c (Fig. 3E & 3F).

To illustrate the role of specific transcription factor XBP1 in ER stress pathway, XBP1 was examined both in FA-induced HHL-5 cells and NAFLD rats. SFN attenuated the expressions of XBP1 mRNA (Fig. 3G) and XBP1 protein (Fig. 3H), with comparable effects to PPC treatment. Similarly, in the FAs-induced cell model, SFN down-regulated the XBP1 expression (Fig. 3I&J).

3.3 SFN protected the structure of ER and attenuated LDs formation

As the key organelle for lipid synthesis, excess lipid accumulation contributes to the morphological aberrance of the ER. HFD accelerates the excessive LDs formation (gray round areas) and accumulation in

hepatocytes (Fig. 4). However, SFN treatment, to some extent, appeared to reduce the LDs accumulation with less grey areas (Fig. 4A). High doses of SFN diminished the LD accumulation as with PPC group. Under physiological conditions, ER is arranged as slim bundle. However, HFD increased the space between rough ERs and induced ER swelling which was exhibited by the longer perimeter of the ER than that following SFN treatment. SFN shortened the distance between the ERs, and the particles on the ER were clearly visualized, which implied that SFN can protect the ER.

To further quantify the structural changes of the ER during NAFLD, the perimeter of the ER was calculated by the free-hand tools using ImageJ software. HFD lengthened the perimeter of the ER, indicating ER swelling (Fig. 4B). SFN in turn decreased the perimeter of the ER (90-160 μm) suggesting the protection of the ER by SFN. In order to illustrate the role of PERK in the ER stress pathway, PERK was examined in both FA-induced HHL-5 cells and NAFLD rats. SFN attenuated the expressions of PERK mRNA (Fig. S1A) and PERK protein (Fig. S1B) especially in the high dose group with effects comparable to PPC treatment. Similarly, in the FAs-induced cell model, SFN (10 μmol/L and 20 μmol/L) down-regulated the PERK expression (Fig. S1C&D).

3.4 SFN prevented the formation of LDs in an XBP1-dependent way

To clarify the key roles of XBP1and SREBP1 during the formation of LDs, a series of dynamic and continuous experiments in HHL-5 cells were performed. After pre- treatment with SFN (10 μmol/L) for 24 h, HHL-5 cells were exposed to FA (250 μmol/L) for 0h, 12h, 24h, 3d, 5d respectively and then harvested for determination. TG content rose slowly after incubation with FAs for 24 h and at this time, no visible LDs were found (Fig. 5A). After 3 days, TG content increased significantly with red LDs visible in the cytoplasm (Fig. 5B). However, pre-protection with SFN significantly decreased the concentration of TG in comparison to FA treatment alone. After 5 days, the red LDs could be more clearly visualized in the FA-treated group. However, the color of red LDs was much lighter and the number of LDs also appeared to decrease after exposure to SFN.

The LD formation and TG synthesis rose in time-dependent manner together with XBP1 mRNA expression. After exposure to FAs for 24 h, XBP1 mRNA expression rose linearly until to the 5th day (Fig. 5C). SREBP1 mRNA expression rose linearly after exposure to FAs for 12h until to the 3rd day. However, SFN (10 μmol/L) reduced both XBP1 and SREBP1 mRNA after 24h (Fig. 5C & 5D). Normal rough ER

appears as bundle and with ribosome attached on it, but fatty acids lead to ER swelling and SFN improved this situation. SFN also decreased the number of LDs (Fig. 5E).

To illustrate the roles of ERS in the development of LDs and to clarify if the down regulations of XBP1 & SREBP1 mRNA by SFN were both linked with the ERS, 4-PBA, the specific inhibitor of ER stress, was used [20]. 4-PBA is supposed to interact with hydrophobic domains of mis-folding proteins and thus prevents their aggregation, which give the chances for correct folding proteins. The number of red LDs stained by Oil-Red was increased in the FA-treated group, whereas 4-PBA reduced the number of LDs with light red (Fig. 5E). SFN also had a similar effect on the number of LDs (Fig. 5F). Additionally, the TG content was decreased in the 4-PBA group compared to the FA-treated group, which suggested that 4-PBA could reduce lipid synthesis (Fig. 5G). Both 4-PBA and SFN treatments attenuated the expressions of XBP1 mRNA (Fig. 5H). However, unexpectedly, 4-PBA, unlike SFN, could not block the increased-expression of SREBP1 mRNA by FAs (Fig. 5I).

Discussion

The current study has shown that SFN exhibits a protective effect on abnormal lipid metabolism both *in vitro* and *in vivo*. SFN protected the structure of the ER when stressed by excessive lipid accumulation and inhibited the expressions of key lipogenic enzymes including ACC, SCD1 and FAS. Moreover, XBP1 and SREBP, two ER stress-associated transcriptional factors, were involved in this process.

A high-fat diet was identified as an activator of ER stress in liver. Recently, ER stress response was identified as a crucial mechanism in a variety of liver disorders including NAFLD [21]. Thapsigargin and tunicamycin, the two pharmacologic ER stress inducers, lead to hepatic lipid accumulation in mice [22]. Moreover, thapsigargin can activate SREBP- 1c followed by an increase in hepatic lipogenesis [23]. In accordance with this, induction of PERK-peIF2α branch in response to ER stress enhances lipid accumulation through SREBP-1c activation in hepatocytes [24]. Conversely, these results showed that SREBP1c expression was not controlled by the ERS. Moreover, the ERS was not a major/significant factor in the downregulation of SREBP1c by SFN. SREBP-1c is one of the transcription factors controlling the hepatic lipid metabolism through the regulation of the expression of critical enzymes involved in glycolytic and lipogenic pathways such as FAS, HMG-CoA synthase (HMGCS) and HMG-CoA reductase (HMGCR) [25]. It should be noted that SREBP-1c also responds to insulin signal and is essential for

glucose carbon utilization and storage. Consequently, it is important to understand whether the activation of SREBP-1c contributes to the insulin signal which is sensitive to the high fat diet. The level of insulin in serum was measured and showed that SFN has a potential to stimulate insulin (data not shown). It is thus speculated that inhibitory expression of SREBP-1c may be largely associated with insulin secretion after SFN treatment [26].

In contrast, XBP1 is newly identified as a transcription factor governing hepatic lipogenesis. [27] XBP1 is a key regulator of the mammalian unfolded protein response (UPR) or ERS response [28]. Upon ER stress, the proximal sensor and endoribonuclease IRE1α induces unconventional splicing of XBP1 mRNA to generate a mature mRNA encoding an active transcription factor, XBP1s, which directly binds to the promoter region of ER chaperone genes [29-31]. XBP1 deficiency weakened *de novo* hepatic lipid synthesis which lead to the concomitant decreases in serum TG, cholesterol and free fatty acids without causing hepatic steatosis [27]. In this study, XBP1 expression are accompanied with the dynamic processes of lipid droplet formation which implied its key role in regulating the TG synthesis. Critical lipogenic genes regulated by XBP1 include SCD1, diacyl glycerol acetyltransferase 2 (DGAT2), and acetyl CoA carboxylase [32-34]. It should be noted that XBP1 regulates the expression of a subset of lipogenic genes in a SREBP- independent manner. As a result, the inhibitory expression of ACC1 and SCD1 by SFN may be mainly mediated by XBP1. Moreover, other animal studies also suggest that SFN regulates lipid metabolism via the 5' AMP-activated protein kinase (AMPK) signalling pathway and ACC1[35]. These studies do suggest that dietary broccoli may alter lipogenesis pathways, consistent with our observation.

Conclusion

It has been demonstrated that SFN improved the abnormal metabolism of lipid both *in vivo* and *in vitro* through targeting the ERS response pathways. SFN suppressed the lipid accumulation in two distinguished manners involving both ERS-dependent XBP1/ACC &SCD1 and ERS-independent SREBP1/FAS pathways.

Acknowledgement

This work is funded by the National Natural Science Foundation of China (No. 81573135). We also thanked Mr. Jim Bacon for the critical reading of the manuscript.

References

[1] Puppala, J., Siddapuram, S. P., Akka, J., Munshi A., Genetics of nonalcoholic Fatty liver disease: an overview. *J Genet Genomics*. 2013, 40, 15-22.

[2] Daniels, T. F., Killinger, K. M., Michal, J. J., Wright, R. W. J., Jiang Z., Lipoproteins, cholesterol homeostasis and cardiac health. *Int J Biol Sci.* 2009, 5, 474-488.

[3] Pagliassotti, M. J., Endoplasmic Reticulum Stress in Nonalcoholic Fatty Liver Disease. *Annu Rev Nutr.* 2012, 32, 17-33.

[4] Fu, S., Watkins, S. M., Hotamisligil, G. S., The Role of Endoplasmic Reticulum in Hepatic Lipid Homeostasis and Stress Signaling. *Cell Metab.* 2012, 15, 623-634.

[5] Ota, T., Gayet, C., Ginsberg, H. N., Inhibition of apolipoprotein B100 secretion by lipid-induced hepatic endoplasmic reticulum stress in rodents. *J. Clin. Invest.* 2008, 118, 316–332.

[6] Walter, P., and Ron, D., The unfolded protein response: from stress pathway to homeostatic regulation. *Science.* 2011, 334, 1081–1086.

[7] Malhotra, J. D., Kaufman, R. J., The endoplasmic reticulum and the unfolded protein response. Semin. *Cell Dev. Biol.* 2007, 18, 716–731.

[8] Choi, Y. J., Shin, H. S., Choi, H. S., Park, J. W., Jo, I., Oh, E. S., Lee, K. Y., Lee, B. H., Johnson, R. J., Kang, D. H., Uric acid induces fat accumulation via generation of endoplasmic reticulum stress and SREBP-1c activation in hepatocytes. *Lab Invest.* 2014, 94, 1114-1125.

[9] Oyadomari, S., Harding, H. P., Zhang, Y., Oyadomari, M., Ron, D., Dephosphorylation of translation initiation factor 2alpha enhances glucose tolerance and attenuates hepatosteatosis in mice. *Cell Metab* 2008, 7, 520–532.

[10] Mirmiran, P., Bahadoran, Z., Golzarand, M., Shiva, N., Azizi, F., Association between dietary phytochemical index and 3-year changes in weight, waist circumference and body adiposity index in adults: Tehran Lipid and Glucose study. *Nutr Metab (Lond).* 2012, 9, 108-116.

[11] Hu, R., Xu, C., Shen, G., Jain, M. R. Khor, T. O., Gopalkrishnan, A., Lin, W., Reddy, B., Chan, J. Y., Kong, A. N., Gene expression profiles induced by cancer chemopreventive isothiocyanate sulforaphane in the liver of C57BL/6J mice and C57BL/6J/Nrf2 (-/-) mice. *Cancer Lett.* 2006, 243, 170-192.

[12] Baek, S. H., Park, M., Suh, J. H., Choi, H. S., Protective effects of an extract of young radish (Raphanus sativus L.) cultivated with sulfur (sulfur-radish extract) and of sulforaphane on carbon tetrachloride-induced hepatotoxicity. *Biosci Biotechnol Biochem.* 2008, 72, 1176-1182.

[13] Yung, C., Matthew, A. W., Elizabeth, H. J., Dietary broccoli lessens development of fatty liver and liver cancer in mice given diethylnitrosamine and fed a western or control diet. *J Nutr.* 2016, 146, 542-550.

[14] Karaskov, E., Scott, C., Zhang, L., Teodoro, T., Ravazzola, M., Volchuk, A., Chronic palmitate but not oleate exposure induces endoplasmic reticulum stress, which may contribute to INS-1 pancreatic cell apoptosis. *Endocrinology.* 2006, 147, 3398-3407.

[15] Wen, L., Aswin, L., Menke, A. D. Koek, G. H., Lindeman, J. H., Stoop, R., Havekes, L. M., Kleemann, R., van den Hoek, A. M., Establishment of a General NAFLD Scoring System for Rodent Models and Comparison to Human Liver Pathology. *PLOS ONE.* 2014, 9, e115922.

[16] He, C., Li, B., Song, Wei., Ding, Z., W, S., Shan Y., Sulforaphane attenuates homocysteine-induced endoplasmic reticulum stress through Nrf-2-driven enzymes in immortalized human hepatocytes. *Agric. Food Chem.,* 2014, 62, 7477-7485.

[17] Arruda, A. P., Pers, B. M., Parlakgül, G., Güney, E., Inouye, K., Hotamisligil, G. S., Chronic enrichment of hepatic ER-mitochondria contact sites leads to calcium dependent mitochondrial dysfunction in obesity. *Nat Med.* 2014, 20, 1427-1435.

[18] Shao, M., Shan, B., Liu, Y., Deng, Y., Yan, C., Wu, Y., Mao, T., Qiu, Y., Zhou, Y., Jiang, S., Jia, W., Li, J., Rui, L., Yang, L., Liu, Y., Hepatic IRE1a regulates fasting-induced metabolic adaptive programs through the XBP1s-PPARa axis signaling. *Nat Commun.* 2014, 27, 3528. doi: 10.1038/ncomms4528.

[19] Josekutty, J., Iqbal, J., Iwawaki, T., Kohno, K., Hussain, M. M., Microsomal Triglyceride Transfer Protein Inhibition Induces Endoplasmic Reticulum Stress and Increases Gene Transcription via Ire1/cJun to Enhance Plasma ALT/AST. *J Biol Chem.* 2013, 288, 14372-14383.

[20] Su, L., Chen, X., Wu, J., Galangin inhibits proliferation of hepatocellular carcinoma cells by inducing endoplasmic reticulum stress. *Food Chem Toxico.* 2013, 62, 810-816.

[21] Ozcan, U. Cao, Q., Yilmaz, E., Lee, A. H., Iwakoshi, N. N., Ozdelen, E., Tuncman, G., Görgün, C., Glimcher, L. H., Hotamisligil, G. S., Endoplasmic reticulum stress links obesity, insulinaction, andtype 2 diabetes, *Science.* 2004,306, 457-461.

[22] Jo, H., Choe, S. S., Shin, K. C., Jang, H., Lee, J. H., Seong, J. K., Back, S. H., Kim, J. B., Endoplasmic reticulum stress induces hepatic steatosis via increased expression of the hepatic very low-density lipoprotein receptor. *Hepatology.* 2013, 57, 1366-1377.

[23] Lee, J. N., Ye, J., Proteolytic activation of sterol regulatory element-binding protein induced by cellular stress through depletion of Insig-1. *J. Biol. Chem.* 2004, 279, 45257–45265.

[24] Bobrovnikova-Marjon, E. Hatzivassiliou, G., Grigoriadou, C., Romero, M., Cavener, D. R., Thompson, C. B., Diehl, J. A., PERK-dependent regulation of lipogenesis during mouse mammary gland development and adipocyte differentiation. *Proc. Natl. Acad. Sci. USA.* 2008, 105, 16314-16319.

[25] Horton, J. D., Goldstein, J. L., Brown, M. S., SREBPs: activators of the complete program of cholesterol and fatty acid synthesis in the liver. *J Clin Invest.* 2002, 109, 1125-1131.

[26] Fu, J., Zhang, Q., Woods, C. G., Zheng, H. Yang, B., Qu, W., Melvin, E. A., Jingbo, P., Divergent effects of sulforaphane on basal and glucose-stimulated insulin secretion in β-cells: role of reactive oxygen species and induction of endogenous antioxidants. *Pharm Res.* 2013, 30, 2248-2259.

[27] Lee, A. H., Scapa, E. F., Cohen, D. E., Glimcher LH. Regulation of hepatic lipogenesis by the transcription factor XBP1. *Science.* 2008, 320, 1492–1496.

[28] Ron, D., Walter, P., Signal integration in the endoplasmic reticulum unfolded protein response. *Nat. Rev. Mol. Cell Biol.* 2007, 8, 519-529.

[29] Shaffer, A. L., Shapiro-Shelef, M., Iwakoshi, N. N., Lee, A. H., Qian, S. B., Zhao, H., Yu, X., Yang, L., Tan, B. K., Rosenwald, A., Hurt, E. M., Petroulakis, E., Sonenberg, N., Yewdell, J. W., Calame, K., Glimcher, L. H., Staudt, L. M., XBP1, downstream of Blimp-1, expands the secretory apparatus and other organelles, and increases protein synthesis in plasma cell differentiation. *Immunity.* 2004, 21, 81-93.

[30] Lee, A. H., Iwakoshi, N. N., Glimcher, L. H., XBP-1 regulates a subset of endoplasmic reticulum resident chaperone genes in the unfolded protein response. *Mol Cell Biol.* 2003, 23, 7448-7459.

[31] Acosta-Alvear, D., Zhou, Y., Blais, A., Tsikitis, M., Lents, N. H., Arias, C., Lennon, C. J., Kluger, Y., Dynlacht, B. D., XBP1 controls diverse cell type- and condition-specific transcriptional regulatory networks. *Mol Cell.* 2007, 27, 53-66.

[32] Abu-Elheiga, L., Oh, W., Kordari, P., Wakil, S. J., Acetyl-CoA carboxylase 2 mutant mice are protected against obesity and diabetes induced by high-fat/high-carbohydrate diets. *Proc Natl Acad Sci U S A.* 2003, 100, 10207-10212.

[33] Ntambi, J. M., Miyazaki, M., Stoehr, J. P., Lan, H., Kendziorski, C. M., Yandell, B. S., Song, Y., Cohen, P., Friedman, J. M., Attie, A. D., Loss of stearoyl-CoA desaturase-1 function protects mice against adiposity. *Proc Natl Acad Sci U S A*. 2002, 99, 11482-11486.

[34] Yu, X. X., Murray, S. F., Pandey, S. K., Booten, S. L., Bao, D., Song, X. Z., Kelly, S., Chen, S., McKay, R., Monia, B. P., Bhanot, S, Antisense oligonucleotide reduction of DGAT2 expression improves hepatic steatosis and hyperlipidemia in obese mice. *Hepatology*. 2005, 42, 362-371.

[35] Yung, J. C., Angela, D. M., Matthew, A.W., Elizabeth, H. J., Dietary broccoli protects against fatty liver development but not against progression of liver cancer in mice pretreated with diethylnitrosamine. *J Funct Foods*. 2016, 24, 57-62.

Figure Legend

Fig.1 Model development and Treatment. Wistar rats were divided into 6 groups. Except for rats in the negative control, the other rats were fed with high fat diet (HFD) at the beginning of the experiment for ten weeks. And SFN (5, 10, 20 mg/kg) was orally administrated every 2 days from the 1st week to the 10th week. PPC, the clinical drug used for the therapy of NAFLD was implied as the positive treatment group by oral gavage every 2 days from the 2nd day in the first week to the 10th week.

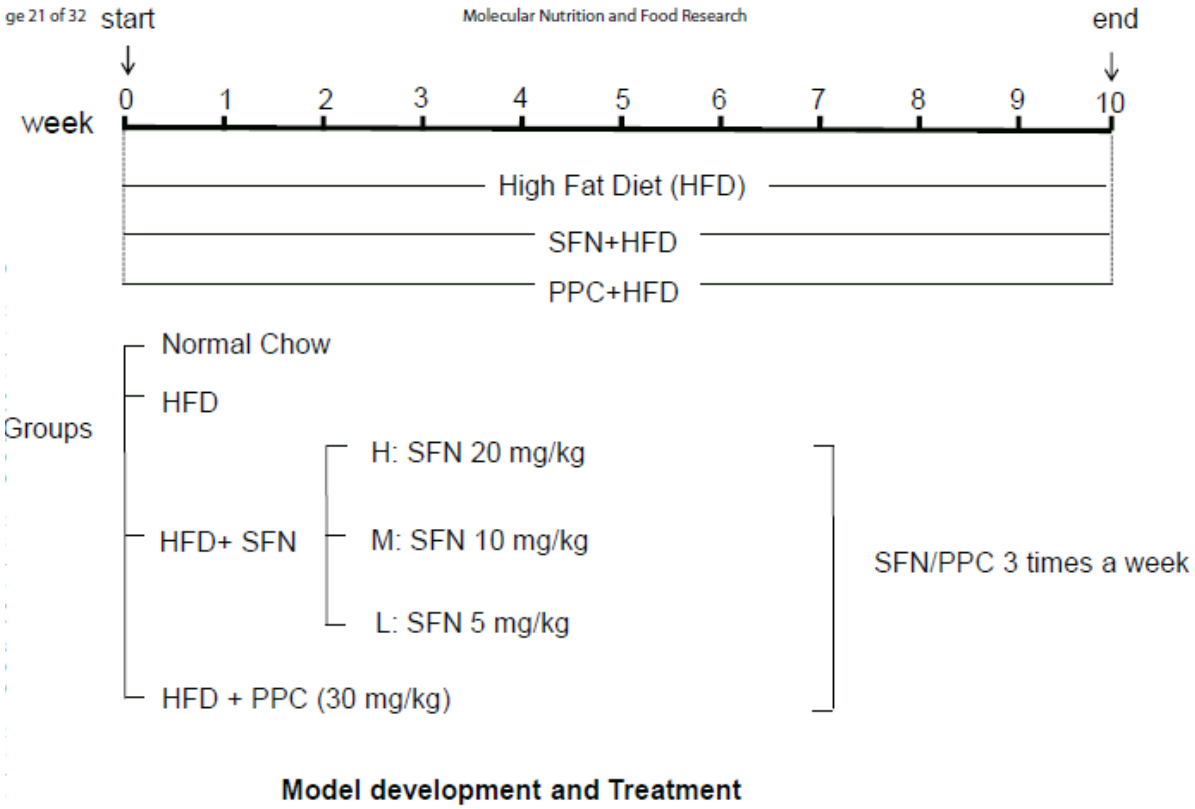

Model development and Treatment

Fig.2 SFN decreased the lipid accumulation in vivo and in vitro. Three doses of SFN (5 mg/kg, 10 mg/kg and 20 mg/kg) and PPC (30 mg/kg) were orally gavaged to rats 3 times a week along with HFD diet. And HHL-5 hepatocytes were pre-treated with SFN (1, 5, 10, 20 μmol/L) for 24 h, followed by 0.25 mmol/L FAs (oleic acid: palmitic acid, 2:1) for 5 days. (A) The content of triglycerides (TG) and cholesterol (TC) in plasma. Data are represented as mean ± SEM (n = 10), significance was analyzed by one-way ANOVA corrected for multiple comparisons with Tukey's test. (B) The content of TG and TC in liver. (C) Pathological examination by H&E staining (400×). White round area as arrow position were LDs. (D) Histological score for lipid accumulation. (E) LDs by Oil-red O staining in HHL-5 hepatocytes (200×). Red round LDs as arrow position were LDs. (F) The concentrations of TG and TC in HHL-5 cells. Data are represented as mean ± SEM (n = 10), significance was determined by one-way ANOVA corrected for multiple comparisons with Tukey's test. Values significantly differ at *P < 0.05, at **P < 0.01, ***P< 0.001 and ****P< 0.0001.

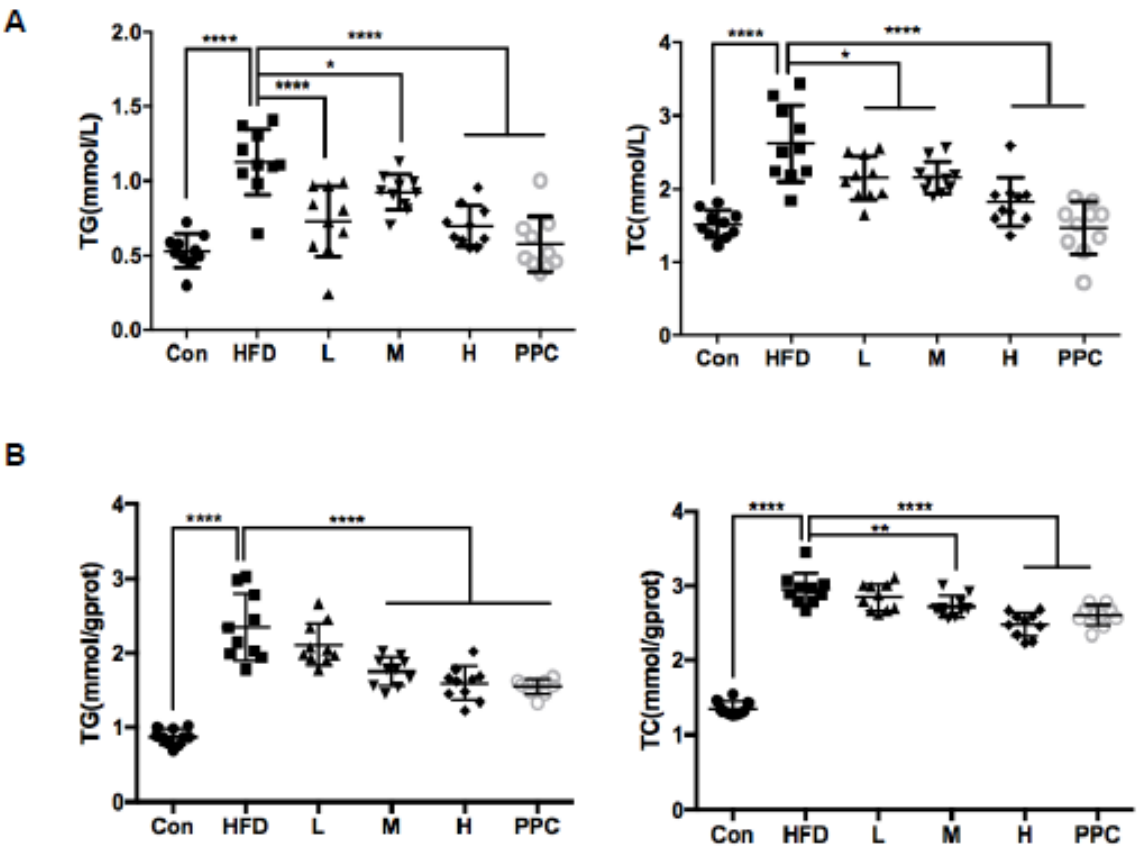

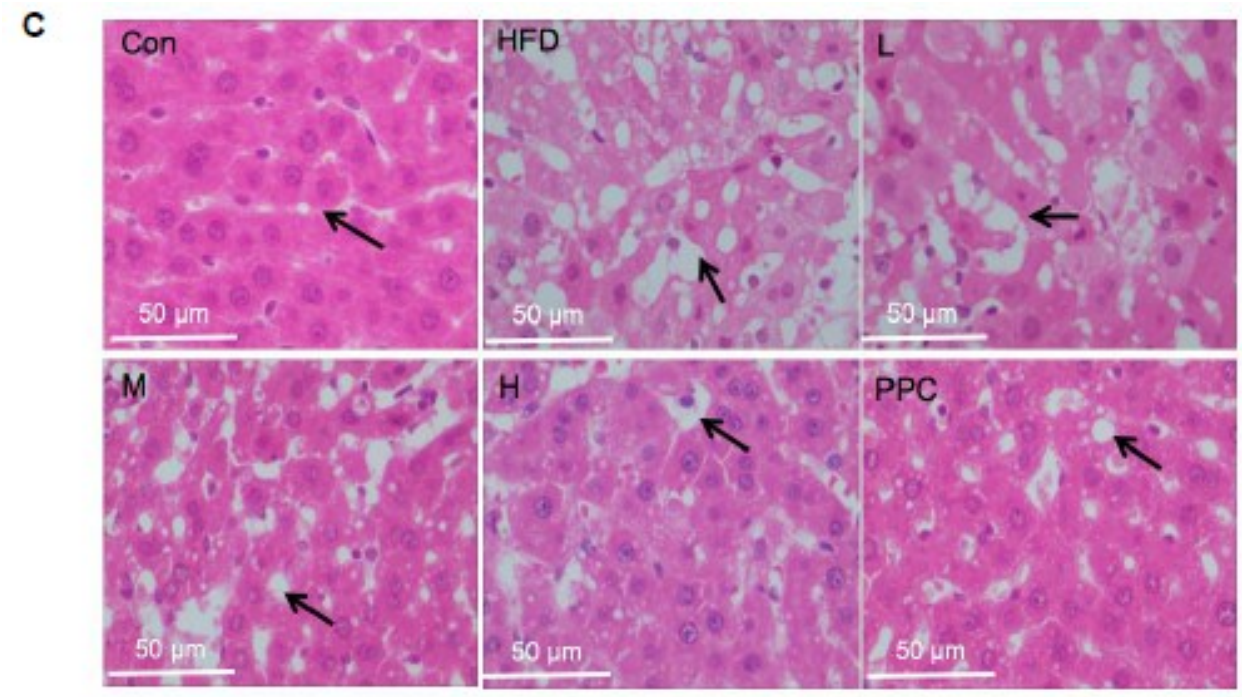

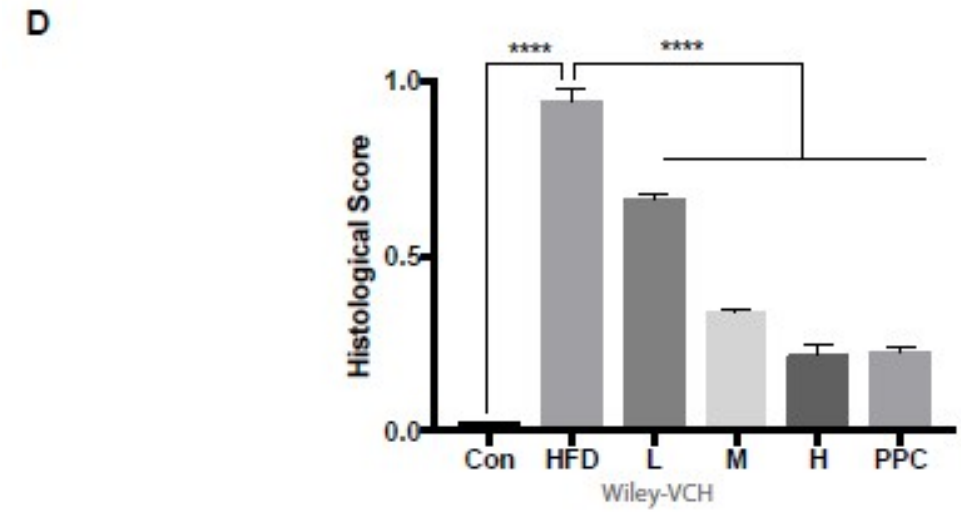

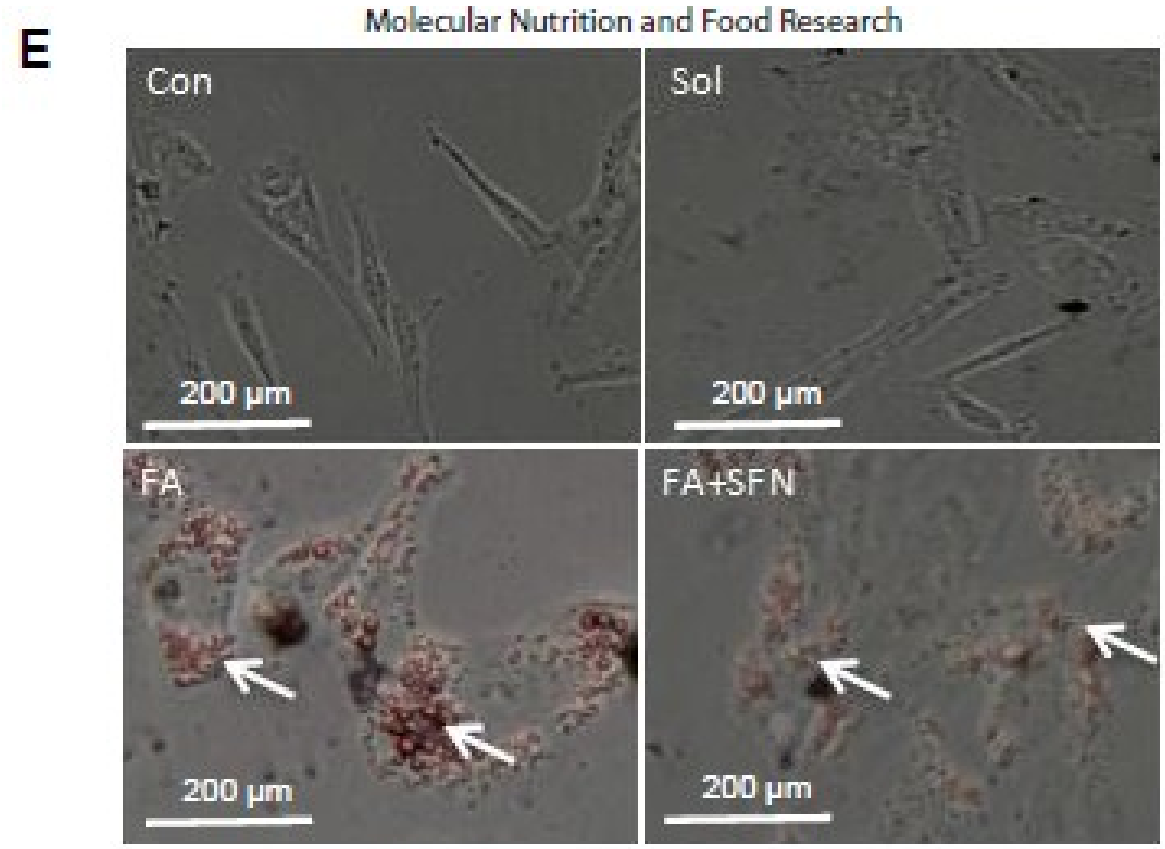

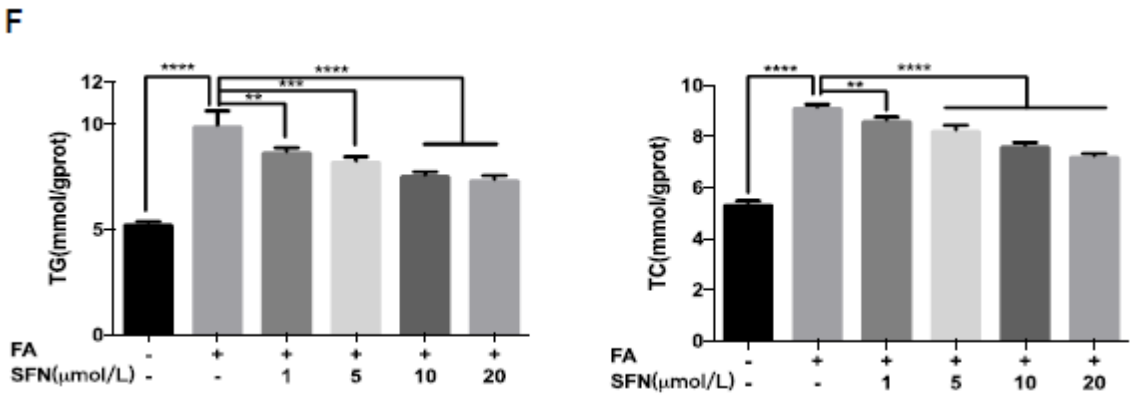

Fig.3 Expressions of lipogenic enzymes and their associated-transcription factors both in rat liver and HHL-5 hepatocytes. Three doses of SFN (5 mg/kg, 10 mg/kg and 20 mg/kg) and PPC (30 mg/kg) were orally gavaged to rats 3 times a week along with HFD diet. And HHL-5 hepatocytes were pre-treated with SFN (1, 5, 10, 20 μmol/L) for 24 h, followed by 0.25 mmol/L FAs (oleic acid: palmitic acid, 2:1) for 5 days. FAS, ACC1 and SCD1 mRNA expression were detected by RT-qPCR both in rat liver (A) and HHL-5 cells (B). SREBP1c expression was measured both in transcriptional (C-liver &E-cells) and translational levels (D-liver &F-cells). XBP1 mRNA expression in liver tissue (G) and in HHL-5 cells (I). XBP1 protein expression was determined by western blot analysis in liver tissue (H) and in HHL-5 cells (J). For rat liver, data are represented as mean ± SEM (n = 10), significance was determined by one-way ANOVA corrected for multiple comparisons with Tukey's test. Values significantly differ at *P < 0.05, at **P < 0.01, ***P< 0.001 and ****P< 0.0001.

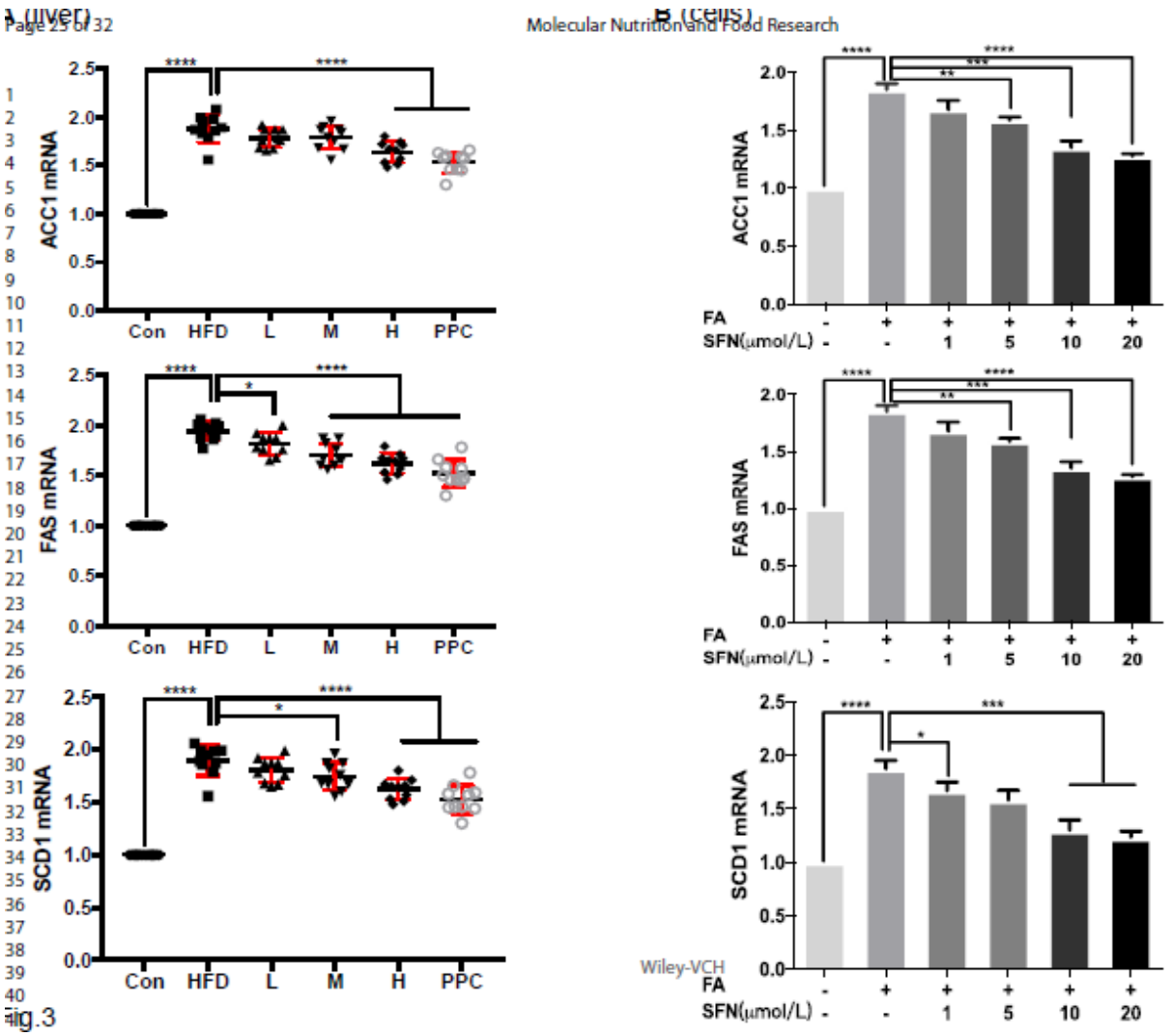

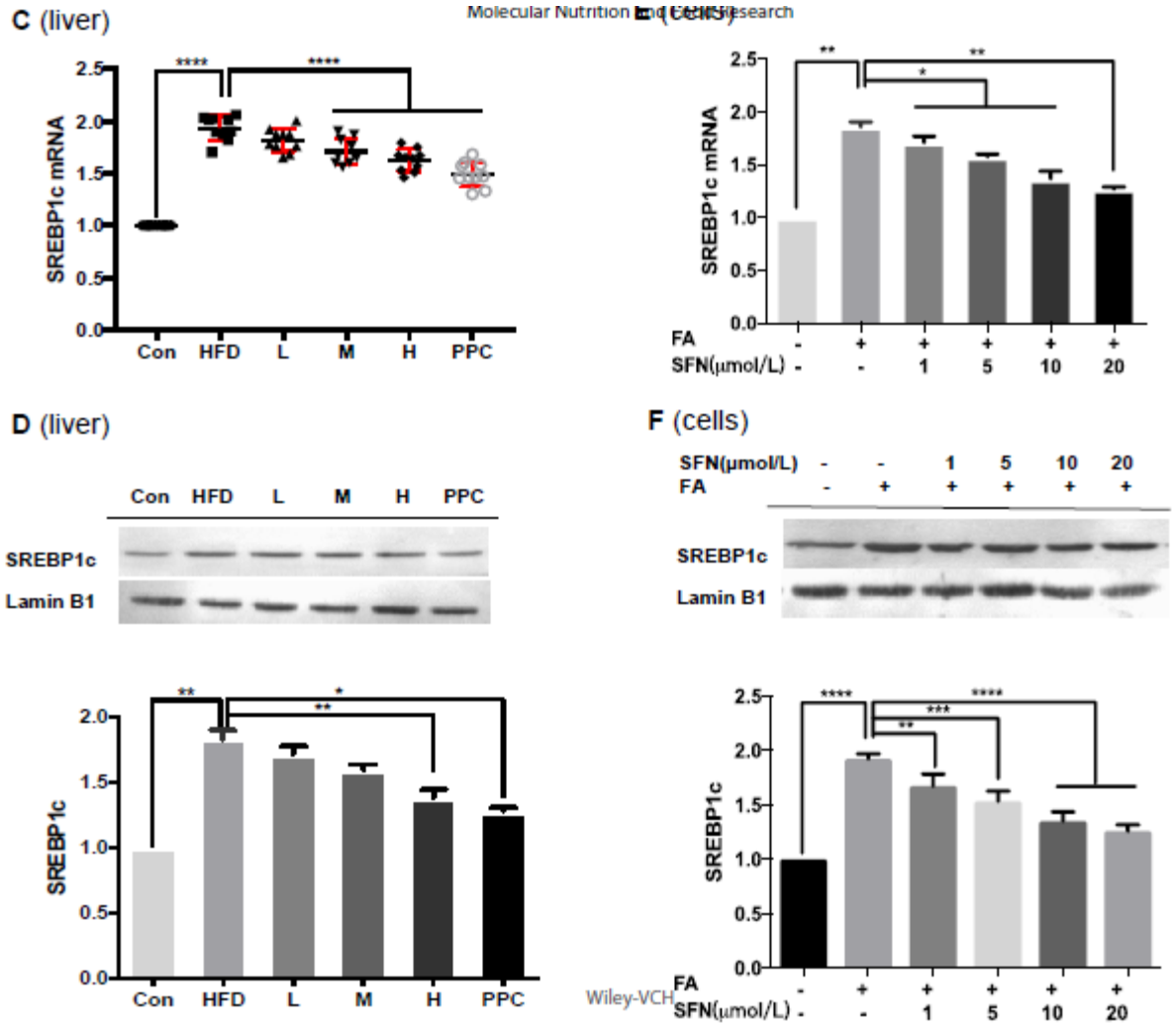

G (liver)

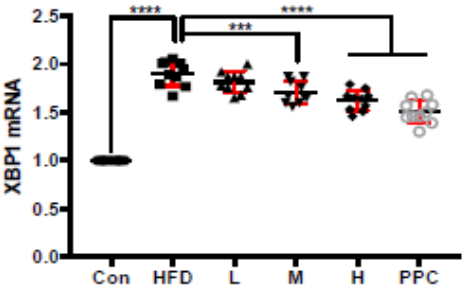

I (cells)

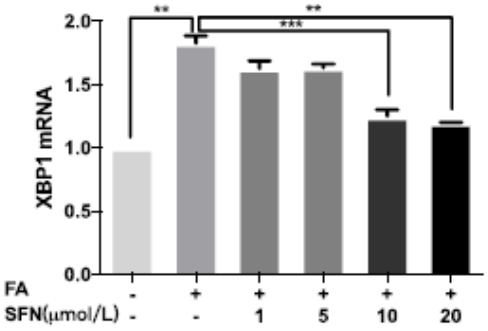

H (liver)

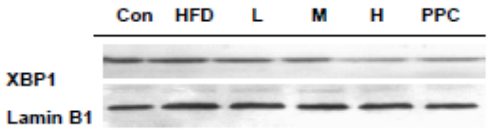

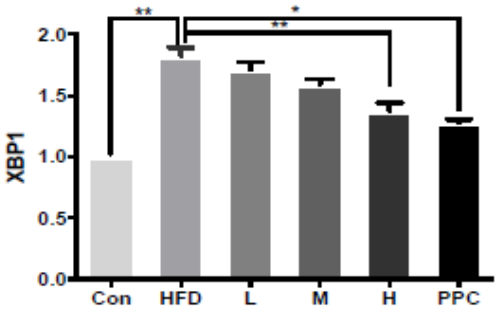

J (cells)

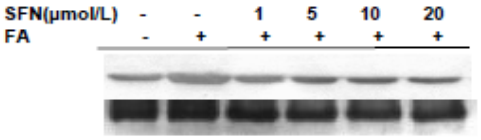

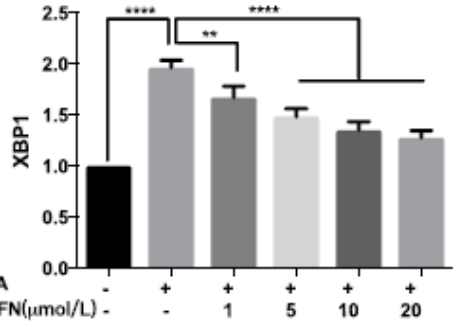

Fig.4 SFN protected the ER stressed by excessive lipid. Three doses of SFN (5 mg/kg, 10 mg/kg and 20 mg/kg) and PPC (30 mg/kg) were orally gavaged to rats 3 times a week along with HFD diet. (A) Organelles structure examined by transmission electron microscopy (10000×)&(20000×). White square area was pointed to the ER and grey round areas were LDs. (B) ER perimeter was measured by free-hand tools (20000×). ER perimeter was calculated by Image J software with the free-hand tools and the length was measured from average of 3 pictures in each experimental group (from 3 different animals per group) according to Hotamisligil's method and all data are mean ± SEM, *P <0.05.

A

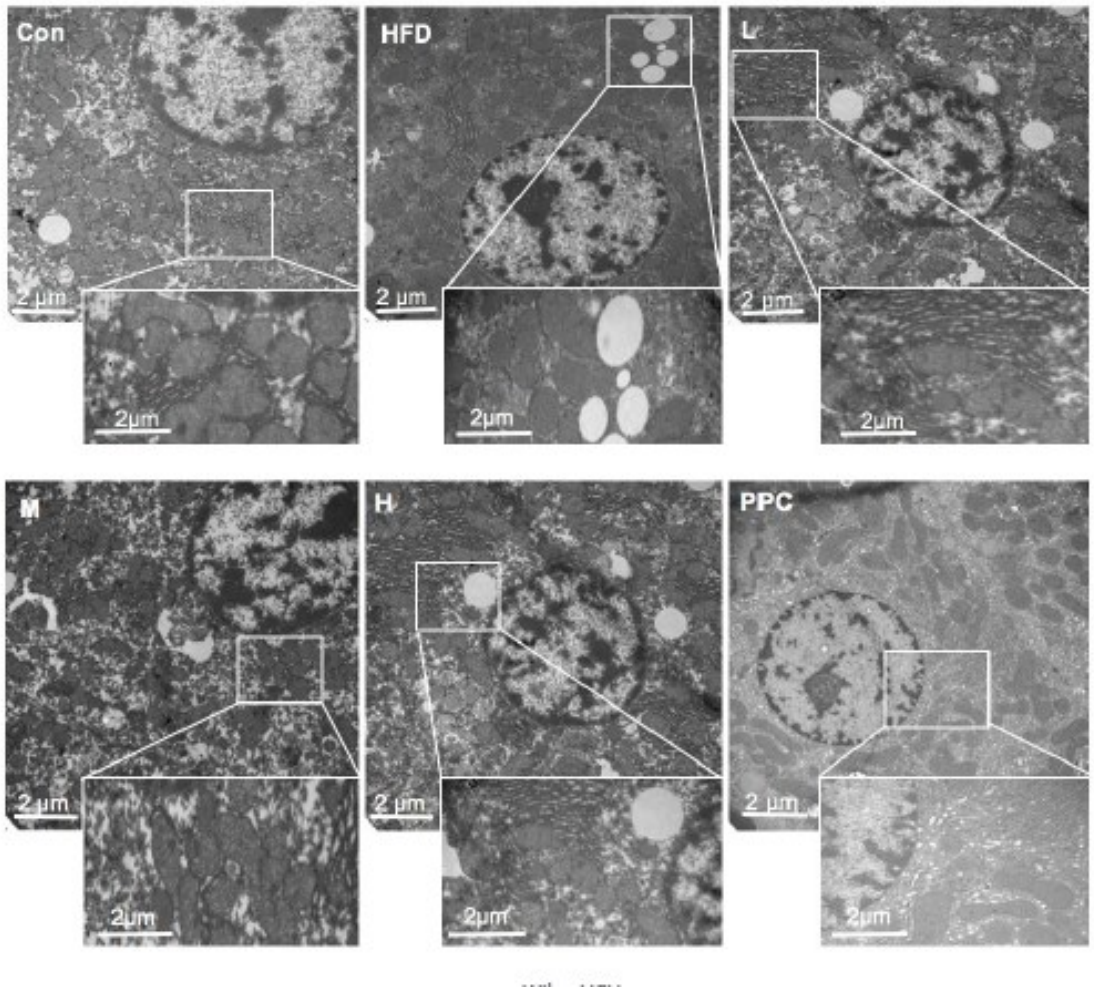

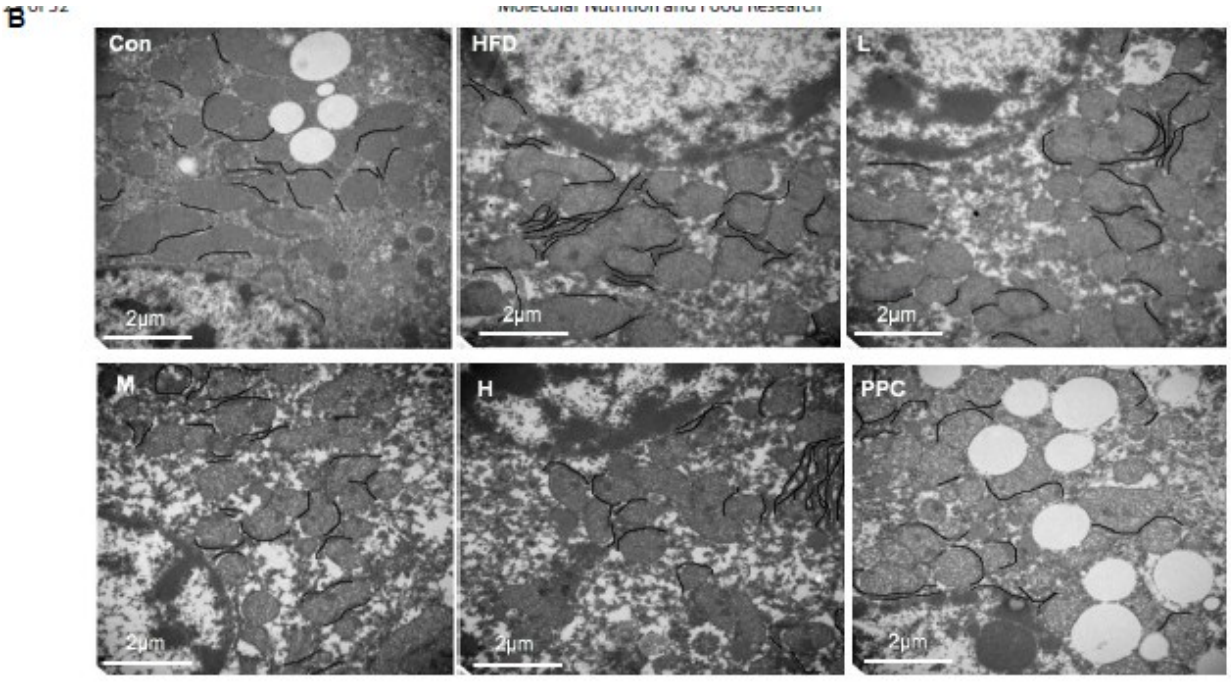

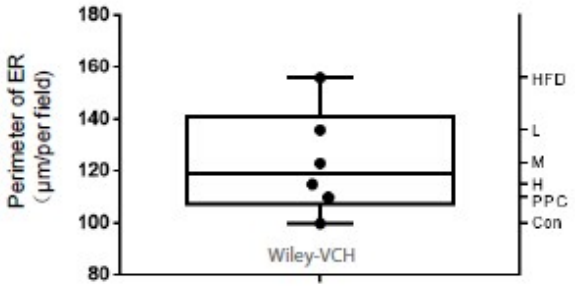

.4

Fig.5 Dynamic formation of lipid droplet induced by FA and inhibition by SFN. After pre- treatment with SFN (10 μmol/L) for 24 h, HHL-5 cells were exposed to FA (250 μmol/L) for 0h, 12h, 24h, 3d, 5d respectively and then harvested for determination. (A) LDs (red round areas) stained by Oil-red during the incubation with FA for desired time (200×). (B) Intercellular concentrations of TG and TC according to time. XBP1 mRNA expression (C) and SREBP1 mRNA expression (D) were determined by real-time PCR analysis. (E) Morphological features of various organelles examined by transmission electron microscopy. Red arrows-Endoplasmic reticulum, blue arrows LDs. (F) Oil-red O staining. Red round areas were LDs. (G) TG content in HHL-5 cells (200×). (H) XBP1 mRNA expression. (I) SREBP1 mRNA expression. Data are represented as mean ± SEM (n = 10), significance was determined by one-way ANOVA corrected for multiple comparisons with Tukey's test. Values significantly differ at *P < 0.05, at **P < 0.01, ***P< 0.001 and ****P< 0.0001.

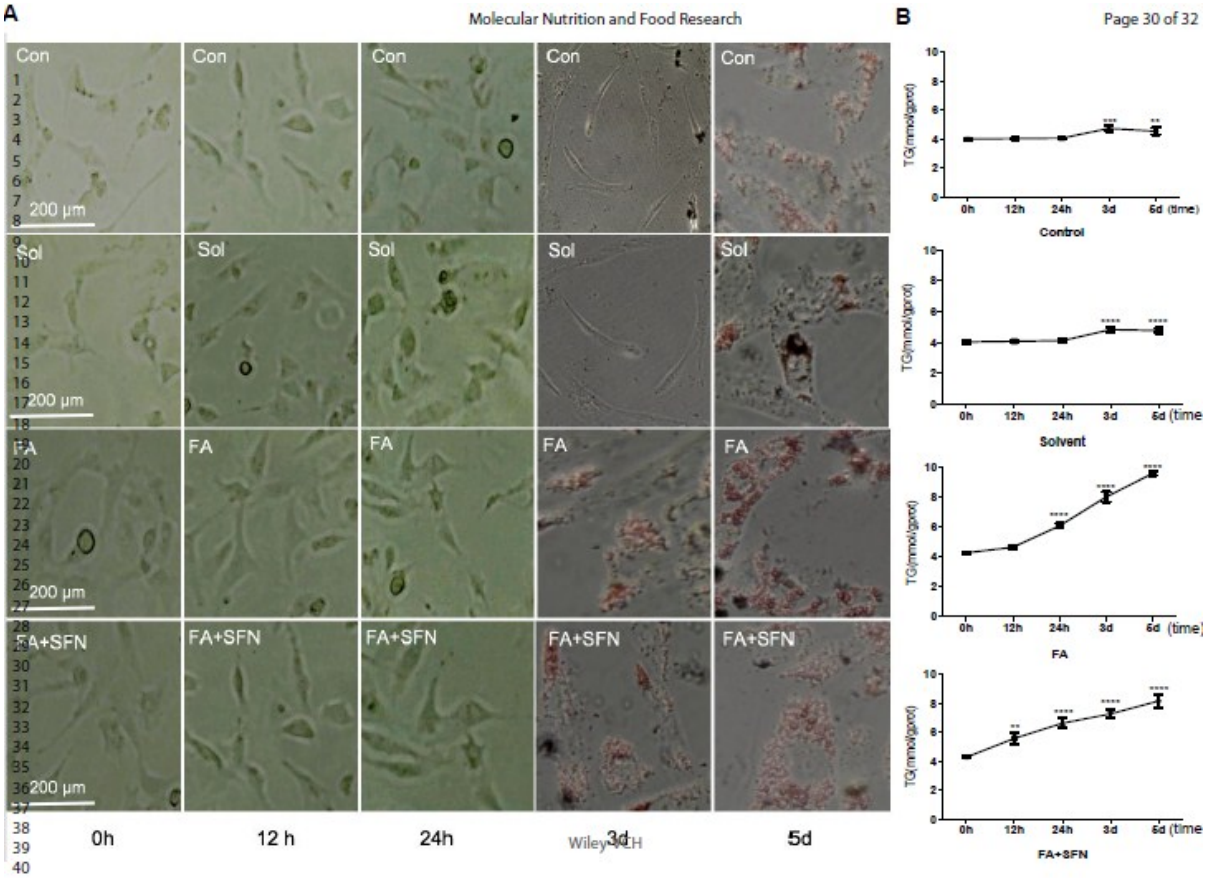

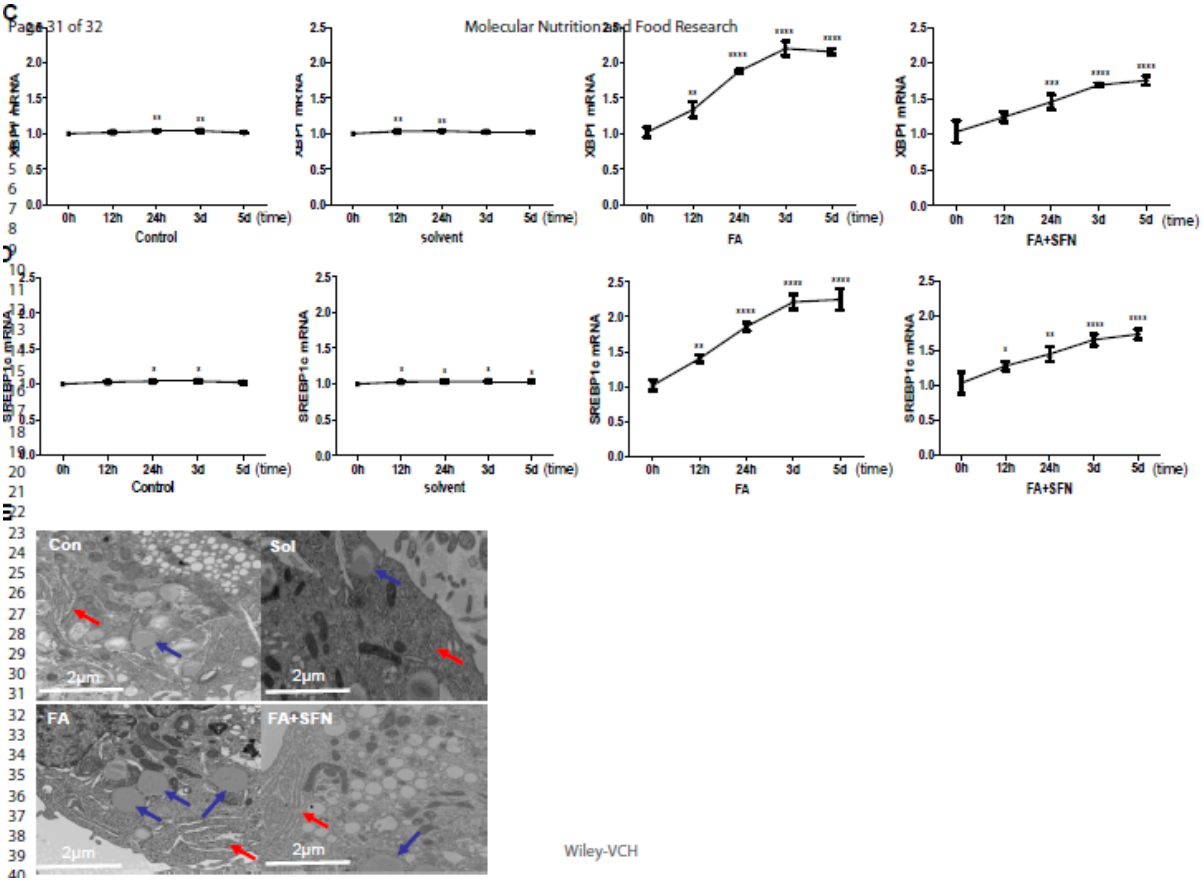

Wiley-VCH

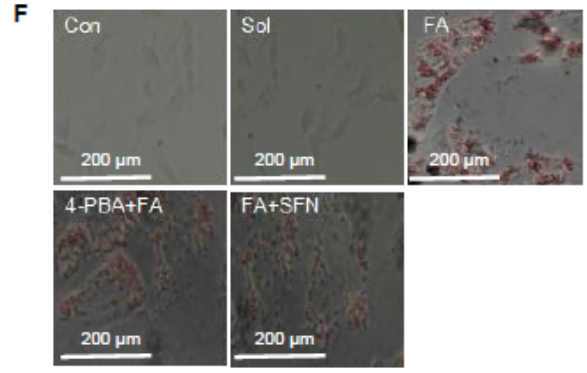

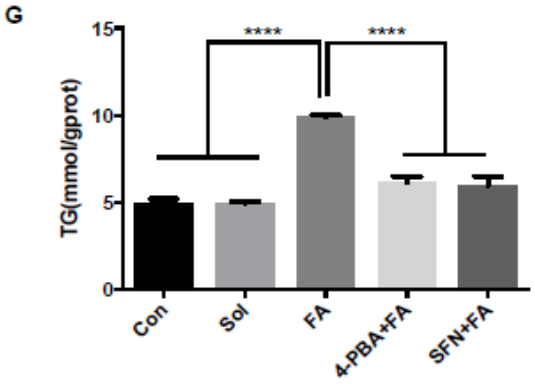

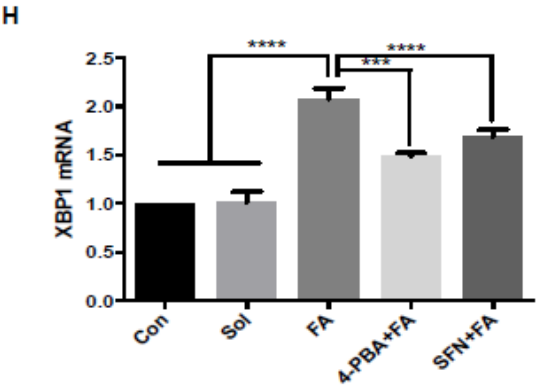

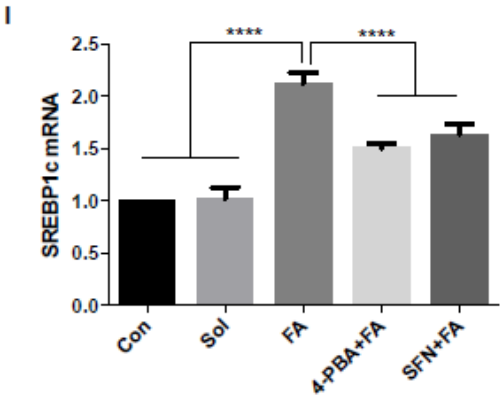

Graphical Abstract

Sulforaphane (SFN) inhibited the lipid synthesis by blocking the endoplasmic reticulum-stress (ERS). On the one hand, SFN suppressed IRE1 and its downstream transcript (sXBP1) which inactivated acetyl CoA carboxylase 1(ACC1) and stearoyl-CoA Desaturase 1 (SCD1). On the other hand, SFN inhibited the expression of SREBP1 through downregulating PERK or stimulating insulin signal, which led to the inhibition of fatty acid synthase (FAS).

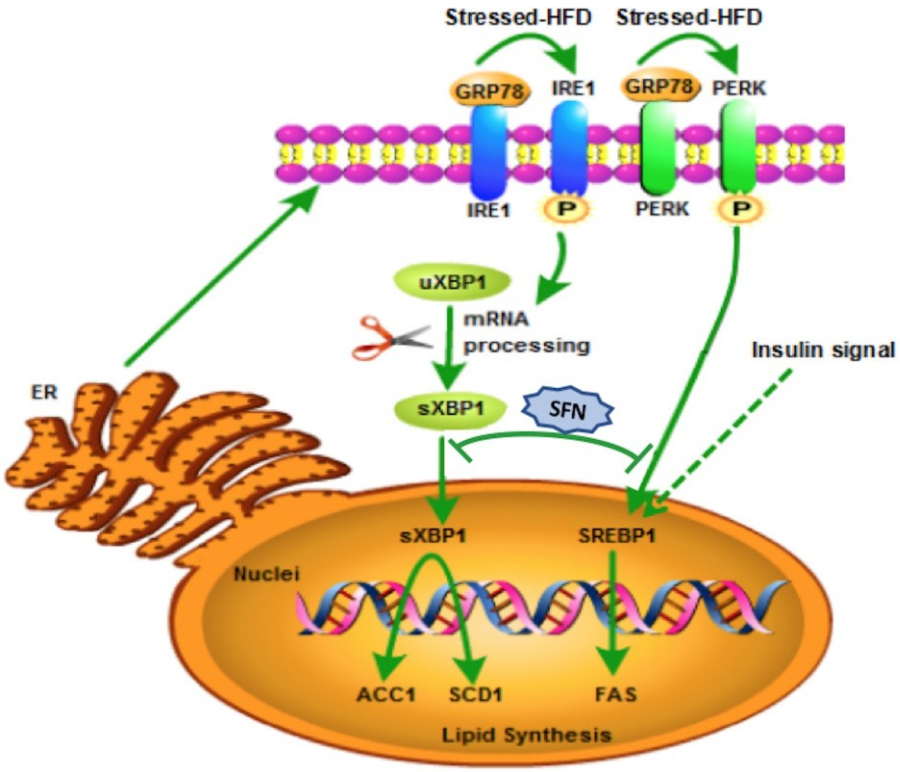

Table 1. Formula of the rodent diet

Ingredient	Normal diet（g/kg）	High fat diet（g/kg）
Casein, 30 Mesh	200	200
L-Cystine	3	3
Corn starch	397	291
Maltodextrin	132	100
Sucrose	100	0
Cellulose	50	50
Soybean Oil	70	25
t- Butylhydroquinone	0.014	0
Mineral Mix	35	10
Vitamin Mix	10	10
Choline Bitartrate	2.5	1
Lard	0	200
DiCalcium Phosphate	0	13
Potassium Bitartrate	0	16.5
Calcium Carbonate	0	5.5
Total kcal	4000	4141

Table 2. PCR primers for rat liver tissue

XBP1	sense 5’-TGGCCGGGTCTGCTGAGTCCG-3’
	antisense 5’-GTCCATGGGAAGATGTTCTGG-3’
PERK	sense 5’-GGCAGGTCCTTGGTAATCAT-3’
	antisense 5’-CCACTGCTTTTTCCCATCAT-3’
SREBP1	sense 5’-TGACCCGGCTATTCCGTGA-3’
	antisense 5’-CTGGGCTGAGCAATACAGTTC-3’
ACC1	sense 5’-GATGAACCATCTCCGTTGGC-3’
	antisense 5’-CCCAATTATGAATCGGGAGTGC-3’
FAS	sense 5’-GGCTCTATGGATTACCCAAGC-3’
	antisense 5’-CCAGTGTTCGTTCCTCGGA-3’
SCD1	sense 5’-AGATCTCCAGTTCTTACACGACCAC-3’
	antisense 5’-GACGGATGTCTTCTTCCAGGTG-3’
β-actin	sense 5’-AGTGTGACGTTGACATCCGTA-3’
	antisense 5’-GCCAGAGCAGTAATCTCCTTCT-3’

Table 3. PCR primers for human hepatocytes

XBP1	sense 5’-CTGGAAAGCAAGTGGTAGA-3’
	antisense 5’-CTGGGTCCTTCTGGGTAGAC-3’
PERK	sense 5’-GAGAAGTGGCAAGAAAAGATGG-3’
	antisense 5’-CTGCGTATTTTAACTGATGGTGC-3’
SREBP1	sense 5’-AGGCCATCGACTACATTCGCTT-3’
	antisense 5’-TCTTCACGCCCTCCATGAGCAC-3’
ACC1	sense 5’-GAGGGAAGGGAATTAGAA-3’
	antisense 5’-ATCACCCCAGGGAGATAC-3’
FAS	sense 5’-GACGTCTGCAAGCCCAAGTA-3’
	antisense 5’-CATCGTCTCCACCAAAATGC-3’
SCD1	sense 5’-GCAGGACGATATCTCTAGCT-3’
	antisense 5’-GTCTCCAACTTATCTCCTCCATTC-3’
β-actin	sense 5’-TTCTGACCCATGCCCAC-3’
	antisense 5’-ATGGATGATATCGCCGCGCTC-3’